J. Phycol. **46,** 66–75 (2010)

DOI: 10.1111/j.1529-8817.2009.00791.x

FIRST HARMFUL *DINOPHYSIS* (DINOPHYCEAE, DINOPHYSIALES) BLOOM IN THE U.S. IS REVEALED BY AUTOMATED IMAGING FLOW CYTOMETRY[1]

Lisa Campbell[2]

Department of Oceanography and Department of Biology, Texas A&M University, College Station, Texas 77843, USA

Robert J. Olson, Heidi M. Sosik

Department of Biology, Woods Hole Oceanographic Institution, Woods Hole, Massachusetts 02543, USA

Ann Abraham

Gulf Coast Seafood Laboratory, U.S. Food and Drug Administration, P.O. Box 158, 1 Iberville Drive, Dauphin Island, Alabama 36528, USA

Darren W. Henrichs

Department of Biology, Texas A&M University, College Station, Texas 77843, USA

Cammie J. Hyatt and Edward J. Buskey

Marine Science Institute, The University of Texas, 750 Channelview Drive, Port Aransas, Texas 78373, USA

Imaging FlowCytobot (IFCB) combines video and flow cytometric technology to capture images of nano- and microplankton (~10 to >100 μm) and to measure the chlorophyll fluorescence associated with each image. The images are of sufficient resolution to identify many organisms to genus or even species level. IFCB has provided >200 million images since its installation at the entrance to the Mission-Aransas estuary (Port Aransas, TX, USA) in September 2007. In early February 2008, *Dinophysis* cells (1–5 · mL^{-1}) were detected by manual inspection of images; by late February, abundance estimates exceeded 200 cells · mL^{-1}. Manual microscopy of water samples from the site confirmed that *D.* cf. *ovum* F. Schütt was the dominant species, with cell concentrations similar to those calculated from IFCB data, and toxin analyses showed that okadaic acid was present, which led to closing of shellfish harvesting. Analysis of the time series using automated image classification (extraction of image features and supervised machine learning algorithms) revealed a dynamic phytoplankton community composition. Before the *Dinophysis* bloom, *Myrionecta rubra* (a prey item of *Dinophysis*) was observed, and another potentially toxic dinoflagellate, *Prorocentrum*, was observed after the bloom. *Dinophysis* cell-division rates, as estimated from the frequency of dividing cells, were the highest at the beginning of the bloom. Considered on a daily basis, cell concentration increased roughly exponentially up to the bloom peak, but closer inspection revealed that the increases generally occurred when the direction of water flow was into the estuary, suggesting the source of the bloom was offshore.

Key index words: **automated; dinoflagellate; early warning; flow cytometry; Gulf of Mexico; harmful algae; imaging; life history; monitoring**

Abbreviations: *cox1*, cytochrome c oxidase I; DSP, diarrhetic shellfish poisoning; DTX-1, dinophysis toxin–1; IFCB, Imaging FlowCytobot; LC–MS/MS (SRM), liquid chromatography–mass spectrometry (selected reaction monitoring); OA, okadaic acid; UTMSI, University of Texas Marine Sciences Institute

Monitoring combined with rapid response has been identified as one of the most effective ways to mitigate the impact of HABs (CENR 2000). Monitoring programs typically rely on manual microscopy for phytoplankton identification, but the levels of expertise and effort required for manual analyses make it difficult to obtain temporal resolution sufficient for early warning and analysis of bloom dynamics. Continuous automated methods can potentially solve this problem; one such approach is imaging-in-flow cytometry. The success of early attempts to use commercially available imaging-in-flow equipment for HAB detection was limited by inadequate image quality and image recognition software, and by rapid fouling (Buskey and Hyatt 2006, Campbell et al. 2008). A new imaging system developed to overcome these limitations, IFCB (Olson and Sosik 2007), is capable of unattended long-duration deployments and produces high-quality images that allow many phytoplankton cells

[1]Received 7 April 2009. Accepted 29 August 2009.
[2]Author for correspondence: e-mail lcampbell@ocean.tamu.edu.

to be identified to genus or even species. In addition, an automated image classifier with accuracy comparable to that of human experts has been demonstrated (Sosik and Olson 2007). Effectiveness and durability have been demonstrated by nearly continuous deployment of an IFCB off the coast of New England since summer 2006 (Sosik et al. 2009).

Our objective was to monitor the phytoplankton in Texas coastal waters, specifically to detect the toxic dinoflagellate *Karenia brevis*, which has been increasing in frequency in this area. Although no *K. brevis* blooms occurred in Texas waters in 2008, the imaging approach revealed a different, unexpected, and also potentially harmful dinoflagellate species. From mid-February to the end of March 2008, *Dinophysis* spp., predominantly *D.* cf. *ovum,* were recorded by IFCB.

Species of *Dinophysis* may produce okadaic acid (OA) and structurally related derivatives known as dinophysis toxins (Yasumoto et al. 1985). These heat-stable and lipophilic toxins are protein phosphatase inhibitors; they are concentrated by filter-feeding bivalves and can cause diarrhetic shellfish poisoning (DSP) in humans. Although DSP is a major concern in Europe and Japan, and several occurrences of *Dinophysis* have been reported for the East Coast of the U.S. (Maranda and Shimizu 1987, Tango et al. 2004), DSP-causing toxins in shellfish have not previously been reported above the action level in the US.

Here, we describe how continuous and automated monitoring provided the necessary information for timely closure of shellfish harvesting, which prevented a potentially large number of cases of human illness from DSP (J. R. Deeds, K. Wiles, G. B. Heideman VI, K. D. White, and A. Abraham, unpublished data). The high temporal resolution and long duration of the observations allowed us to examine factors that could influence population dynamics, including life-history stages (gametes and planozygotes), cell-division rate (based on frequency of dividing cells), and possible prey (*M. rubra*).

MATERIALS AND METHODS

Instrument and deployment. IFCB (Olson and Sosik 2007) captures images of nano- and microplankton (~10 to >100 μm) together with the light scattering and chlorophyll fluorescence associated with each image. The images are of sufficient resolution (1 μm) that many phytoplankton can be identified to genus or even species. IFCB was deployed in the pier laboratory at the University of Texas Marine Sciences Institute (UTMSI), located on the Port Aransas ship channel at the entrance to the Mission-Aransas estuary on the Gulf of Mexico (27.84°N, 97.07°W). Strong currents in the ship channel made submersible deployment difficult, so IFCB was installed in the laboratory at the seaward end of the pier. Seawater was pulled up to the instrument using a peristaltic pump (Model: 85M5; Stenner Pump Company, Jacksonville, FL, USA). The pump was located beyond the IFCB sampling point so sample water did not pass through the pump. The seawater sampling tube (15 m Tygon tube, ID 1/8″) extended to 3 m beneath the water surface at mean tide, and the pumping rate was 90 mL · min^{-1}. Copper screen (1/16″) excluded large particles from the Tygon tubing. Fouling was removed by running bleach through the sample delivery tubing at weekly intervals. The IFCB sample was taken from this flow through PEEK tubing (2 m long, ID 1 mm), with 150 μm nylon screening to prevent larger particles from entering the IFCB. A 5 mL sample was analyzed by IFCB every 20 min; fluorescent standard particles (red fluorescent 9 μm, XPR-1653; Duke Scientific Corp., Palo Alto, CA, USA) were run after every 50th sample. Images were transferred via the Internet for analysis and archiving.

Automated classification and abundance estimates. IFCB images were automatically processed and classified following the approach described in Sosik and Olson (2007). The approach relies on a supervised machine learning algorithm (Support Vector Machine) where training is based on example images categorized by manual inspection. The specific classifier developed in Sosik and Olson (2007) was not applicable to this data set because the community composition was very different. To build a new classifier, training set images for this work were taken from samples drawn intermittently from throughout the Port Aransas time series. Because the resulting number of manually identified categories was large (>40) and our immediate goal was to optimize accurate enumeration of selected categories (i.e., *Dinophysis* spp., *Prorocentrum* spp., *Myrionecta rubra*), we used a modification of Sosik and Olson (2007). For this situation, we constructed a series of ''one-versus-all'' support vector machines, instead of a single multi-class (''one-vs.-one'') classifier. The main advantage of this variant is that it allows us to use different subsets of image features for each classifier, where each subset is optimized for discriminating the corresponding category (from all other categories combined). All images from the time series (unknowns) were evaluated against each resulting classifier; in the case of conflicts (image positively associated with more than one category), final identity was assigned to the category with the highest probability of affiliation. Images that did not have positive affiliation with any of the training set categories were labeled ''other.'' As in Sosik and Olson (2007), final abundance estimates for the categories of interest were determined after correction for classification error rates by implementing the procedure of Solow et al. (2001).

Water sampling. In addition to the IFCB sampling, surface seawater samples were manually collected from the pier, near the intake of the IFCB. On 15 February 2008, a sample was inspected by manual microscopy to verify the presence of *Dinophysis*. On 25 February 2008, replicate aliquots of seawater were preserved with Lugol's iodine for cell counting by manual LM and cytochrome c oxidase I (*cox1)* sequence analysis and frozen for toxin analysis. Additional samples were collected for cell counts only on five dates later in February and March, and two samples archived before 15 February 2008 (for other purposes) were also later inspected for *Dinophysis*.

Manual microscopy. Dinophysis cell abundance in Lugol's iodine-preserved samples was determined using a gridded Sedgewick Rafter chamber (Part# Graticules S52; Pyser-SGI Limited, Faircroft Way, Edenbridge, Kent, UK) and Olympus BX60 compound microscope (Olympus America Inc., Center Valley, PA, USA). The 95% confidence intervals were computed as given in Suttle (1993).

DNA sequence analysis. Species identification was validated by examining mitochondrial *cox1* sequences from Lugol's iodine preserved samples stored at 4°C. Single-cell PCR amplifications ($n = 18$) were performed with the method of Henrichs et al. (2008). The *cox1* primers (Lin et al. 2002) were used as described by Raho et al. (2008). Products were sequenced using ABI PRISM BigDye Terminator and an ABI

3100 Genetic Analyzer (Applied Biosystems, Foster City, CA, USA). Sequences were edited and compared using Sequencher 4.2 (Gene Codes, Ann Arbor, MI, USA).

Sample extraction for toxin analysis. Methanol was added to the sample (500 mL) to give a final methanol concentration of 20%. The mixture was passed through a 10 g Varian C_{18} Mega Bond Elut cartridge (Part# 12256031, Varian, Harbor City, CA, USA). The cartridge was then washed with five void volumes (60 mL) of 20% methanol in water and eluted with 10 void volumes (120 mL) of 100% methanol. The eluate was dried and resolubilized in 500 μL methanol for analysis.

Hydrolysis of esters. For determination of total OA and dinophysis toxin–1 (DTX-1), esters of OA and DTX-1 were base hydrolyzed to free acids following the procedure of McNabb et al. (2005). Twenty-eight microliters of 2.5 M NaOH was added to 200 μL of the extract in methanol:water (9:1) and heated at 76°C for 40 min. The extract was neutralized with addition of 28 μL of 2.5 M acetic acid while cooling in an ice bath. The reaction mixture was diluted 10-fold with 20% methanol in water and applied on a C18 solid phase extraction column. The column was then washed with 5 mL of water, and analytes were eluted with 5 mL of methanol. The eluates were dried and resolubilized in methanol for analysis.

Toxin analysis. Seawater extracts were analyzed at the Gulf Coast Seafood Laboratory using liquid chromatography–mass spectrometry (LC–MS). The LC–MS system consisted of an Agilent 1100 LC system (Agilent Technologies, Palo Alto, CA, USA) coupled to a 4000 QTRAP triple quadrupole/linear ion trap hybrid mass spectrometer (Applied Biosystems—MDS SCIEX) with Turbo-Ion Spray interface. Separations were performed on a Luna C8 (2), 150 × 2.0 mm column (Phenomenex, Torrance, CA, USA) at 40°C. LC mobile phase solvents were water and acetonitrile, containing 0.1% formic acid. The acetonitrile percentages in the gradient were 35% for 2 min, linear gradient to 80% at 30 min, 95% at 35 min, holding at 95% for 10 min, return to 35% at 50 min, and 10 min equilibration before the next injection. MS parameters for selected reaction monitoring (SRM) in positive ion mode; 5 kV capillary voltage; 100 V declustering potential; 400°C source temperature; 35 eV collision energy; precursor/product ion pairs for LC–MS/MS (SRM) for OA, m/z 805.5 → 751.5, m/z 805.5 → 733.5, m/z 805.5 → 715.5, and for DTX-1, m/z 819.5 → 765.5, m/z 819.5 → 747.5, m/z 819.5 → 729.5. Area responses of the three transitions monitored were summed for each compound. OA and DTX-1 reference materials (LC Laboratories, Woburn, MA, USA) were used for identification and quantification.

Oceanographic data. Water depth, salinity, and temperature data were obtained from the Mission–Aransas National Estuarine Research Reserve Centralized Data Management Office (http://cdmo.baruch.sc.edu). Data for current velocity were obtained from the Texas Coastal Ocean Observation Network, Division of Nearshore Research, Conrad Blucher Institute for Surveying and Science, Texas A&M University-Corpus Christi (http://lighthouse.tamucc.edu/overview/109).

Life-history stages. Dinophysis images were manually inspected to quantify the occurrence of various life-history stages. Because this approach required reviewing thousands of images, calculations were only made for selected days. Cell pairs attached lengthwise (presumably at the dorsal megacytic bridge and usually appearing in dorsal or ventral view) were assumed to be undergoing division (Giacobbe and Gangemi 1997, Reguera et al. 2003). We also identified what appeared to be pairs of fusing gametes (cells of unequal size attached at ventral margins or at the apical end) and planozygotes (single cells with two trailing flagella) (Giacobbe and Gangemi 1997, Escalera and Reguera 2008). Images of dividing cells usually showed the paired cells in dorsal or ventral view, while single cells or cells fusing (in the same plane) were almost always in lateral view. This difference is presumably due to the orientation effects of IFCB's rectangular flow cell; dividing cell pairs are not flattened like single or fusing cells and so are less subject to flow orientation.

Analysis of variance over time (comparing 2-week intervals in February and March) was performed with two methods: χ^2 test with Bonferroni correction for multiple comparisons for binomial data (frequency of occurrence) and, in other cases, (time of day of occurrence) F-test with the Tukey's test applied for appropriate multiple comparisons.

Cell-division rate. The cell-division rate of *Dinophysis* was estimated from the frequency of dividing cells evident in manually inspected IFCB images. Cell division was phased (see Results), which allowed us to apply two methods: the $f_{\max}$ method and the mitotic index method (McDuff and Chisholm 1982). When division is synchronized, $f_{\max}$, or maximum in frequency of dividing cells per 24 h period, is related to growth rate (μ):

$$\mu = \ln(1 + f_{\max}) \tag{1}$$

(eq. 3b from McDuff and Chisholm 1982). Note that this approach, which does not require knowledge of the duration of the terminal event, produces an estimate of the minimum growth rate (Vaulot 1992). The mitotic index is used to calculate growth rates from the integrated value of the frequency of division per unit time:

$$\mu = \frac{1}{nt_{\mathrm{d}}} \sum_{i=1}^{n} \ln(1 + f_i), \tag{2}$$

where f_i is the frequency of dividing cells in interval i, and t_d is the duration of the division event (eq. 6b from McDuff and Chisholm 1982, Carpenter and Chang 1988). Since we do not know t_d, we evaluated μ with $t_d = 2$ or 3 h. This range is supported by the temporal distribution of dividing cells observed in our data set (see Results) and also consistent with a previous report for duration of a terminal event including cytokinesis (paired cells) and recently divided cells (cells regenerating the sulcal list) for *D. sacculus* (Garcés et al. 1997).

RESULTS

IFCB was deployed at the UTMSI pier laboratory in September 2007 and produced >200 million images by July 2008 (with 199 d of operation out of 292 d during the period). These observations revealed dramatic changes in phytoplankton community composition; we report here on the subset of the observations that concern a HAB.

In early February 2008, manual inspection of the IFCB images revealed *Dinophysis* cells (Fig. 1) more frequently than observed earlier in the time series, and a water sample collected at the pier on 15 February and examined by manual LM verified the presence of *Dinophysis* spp. The combination of IFCB image acquisition and automated classification revealed a detailed picture of a major bloom over the next few months (Fig. 2). Identification of cells by manual inspection of a subset of IFCB images verified that automated classification with a single error correction matrix was effective for a range of taxa over the entire period from January to May 2008 (Fig. 3). Manual microscopy of a number of independent water samples, including some

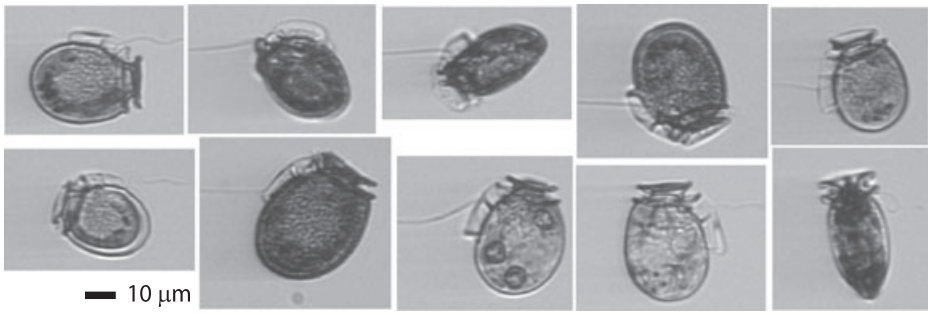

FIG. 1. Selected IFCB images of *Dinophysis* acquired during February and March 2008 in the Port Aransas ship channel show the range of presentations typical in the full data set, which includes ~380,000 *Dinophysis* images. *Dinophysis* cells are laterally flattened, and most IFCB images show the cell's flattened side (due to shear-induced orientation in the rectangular flow cell), but see bottom right for an edge view. Also see Figures 5 and 7 for views of sexual stages and cells with bubble-like structures. IFCB, Imaging FlowCytobot.

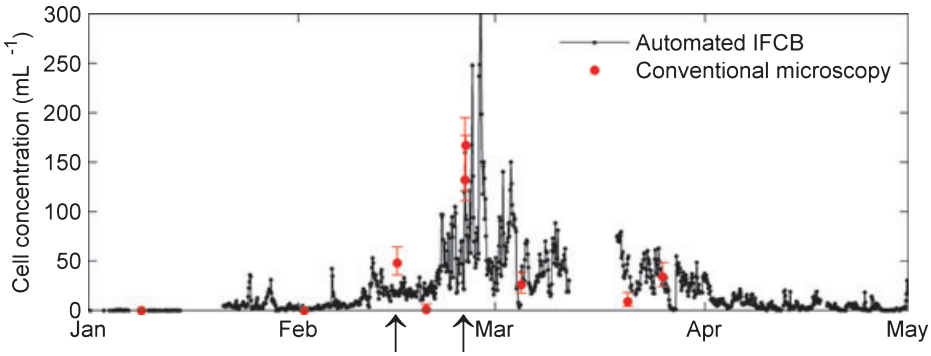

FIG. 2. Time series of *Dinophysis* abundance in the Port Aransas ship channel in early 2008. Automated analysis of IFCB data provided 2 h resolution through most of the 4-month bloom, which was verified with independent samples manually examined by conventional microscopy (±95% confidence intervals). Standard errors for all IFCB data points were <3.6 cells · mL^{-1}, and 80% were <1 cell · mL^{-1} and are omitted from the plot for clarity. Arrows indicate dates when early IFCB results prompted targeted sampling for conventional microscopy (15 February) and toxin assays (25 February). IFCB, Imaging FlowCytobot.

archived from earlier in the season, corroborated the *Dinophysis* bloom pattern (Fig. 2): manual results were not significantly different from those of the automated classifier ($P < 0.05$). Abundance results from the classifier indicated that in January, before the bloom, *Dinophysis* spp. concentrations were 1–5 cells · mL^{-1}; for several weeks during February and March, they exceeded 50 cell · mL^{-1} and at the peak of the bloom exceeded 300 cell · mL^{-1}.

A seawater sample (containing 132 *Dinophysis* cells · mL^{-1}) was collected for toxin analysis on 25 February, after elevated numbers of *Dinophysis* were observed for 2 weeks. OA was detected in the bloom seawater sample, while DTX-1 was not (Fig. S1 in the supplementary material). The concentration of free OA was 5.7 ng · mL^{-1} seawater; after hydrolysis, the concentration increased to 6.9 ng · mL^{-1} seawater, consistent with the presence of esters of OA. These results led to further testing that showed contamination of oysters from the Port Aransas region (J. R. Deeds, K. Wiles, G. B. Heideman VI, K. D. White, and A. Abraham, unpublished data).

Water samples collected at the pier and examined by manual LM showed that the bloom consisted primarily of *D.* cf. *ovum*, although cells resembling *D. acuminata* and *D. fortii* were also present. *D. caudata* appeared at the end of March but was only a small fraction of the total population.

Species identification was also verified from DNA analysis of the pier sample. It was recently noted that species within this *Dinophysis* spp. complex (*D. acuminata*, *D. sacculus*, *D. ovum*) cannot be distinguished based on the LSU or ITS regions, and so the mitochondrial *cox1* gene was proposed as a more informative marker (Raho et al. 2008). Sequence results for the *cox1* region from all 18 individual single cells picked randomly from the sample matched *D. ovum* at all identified positions (GenBank accession no. AM931583). This result was consistent with the sample being dominated by *D. ovum* or *D.* cf. *ovum*.

Dinophysis cell abundance often changed dramatically during a day (Fig. 4), presumably as tides carried different water masses past the sampling point. During the week preceding the bloom peak, current measurements and IFCB observations showed that increasing *Dinophysis* abundances coincided with water movements into the estuary, suggesting that

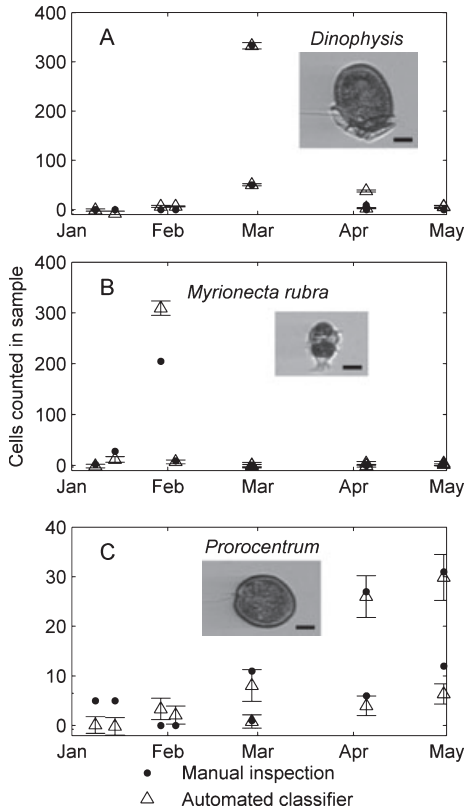

FIG. 3. Cell counts for three taxa observed in selected IFCB samples over the study period. Number of cells counted by manual identification of images is compared with automated classification for 10 samples selected from the time series. (A) *Dinophysis* spp. (B) *Myrionecta rubra*. (C) *Prorocentrum* spp. Scale bars = 10 μm. IFCB, Imaging FlowCytobot.

the bloom originated offshore rather than within the estuary.

Manual inspection of the *Dinophysis* images revealed that dividing cells were most often observed in the morning and that 75% occurred within a 3 h period (Fig. 5, Table 1). Pairs of cells that appeared to be fusing gametes (Escalera and Reguera 2008) were also observed during the morning hours. In contrast, cells with two flagella, possibly planozygotes (as described by Escalera and Reguera 2008), were observed at all times of day. No dramatic changes in the size of *Dinophysis* cells (length or width from automated image analysis) were observed over the course of the bloom (data not shown).

The phasing of cell division allowed population growth rates to be estimated from the frequency of dividing cells; the mitotic index and f_{max} approaches yielded similar estimates of growth rates (Fig. 6) and suggest that growth rates were the highest ($0.2–0.3 \cdot d^{-1}$) in early February. As the bloom progressed and reached its maximum in cell abundance, growth rates declined by >50% and, after the peak abundance, by >90%. These trends are reflected in significant differences in the frequency of dividing cells among 2-week intervals during February and March (Table 1). Fusing gametes were observed at a significantly higher frequency in the first half of February than in the other intervals, which were of similar lower magnitude. Planozygote occurrence showed a similar pattern, except that there was a significantly higher rate in the last half of March than in the preceding month. All differences that were significant were highly so ($P << 0.001$).

In the course of manual inspection to quantify life-history stages, we noted in images from 27 February *Dinophysis* cells with distinctive bubble-like features (Fig. 7). Cells with bubbles were present only during the outgoing tide, when cell concentrations were low; after the current changed direction, cell concentrations increased by an order of magnitude, but cells with bubbles were no longer present.

The IFCB time series observations also revealed ''blooms'' of two other species with possible connections to HABs. Before the toxic event, there was a period with high abundance of the ciliate *M. rubra*, a known prey item for *Dinophysis* (Park et al. 2006) (Fig. 8). *M. rubra* first increased above background levels ($<1 \cdot mL^{-1}$) in mid-January and reached a maximum of ~300 cells $\cdot mL^{-1}$ by the end of January. This peak was short-lived, and after a few days, *M. rubra* abundance decreased to <20 cells $\cdot mL^{-1}$. Another potentially toxic dinoflagellate, *Prorocentrum* spp., reached densities of $100 \cdot mL^{-1}$ in late March; *Prorocentrum* and *Dinophysis* were both present until mid-April (Fig. 8).

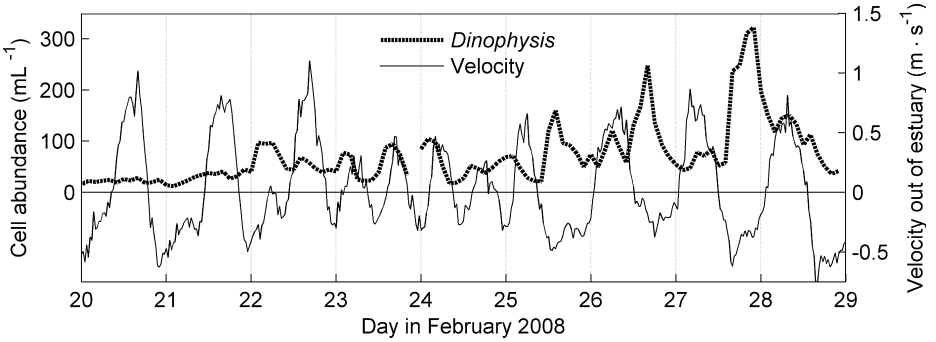

FIG. 4. Hourly resolved *Dinophysis* abundance from IFCB analysis and horizontal currents (positive values indicate flow out of the estuary) during the last 10 d of February. IFCB, Imaging FlowCytobot.

We observed a large range in the size of *M. rubra* cells, with cell widths from 10 to ~30 μm, and the cell size distribution changed as the event proceeded: the population was dominated by large cells during the peak in abundance, but by smaller cells before and after (Fig. 9).

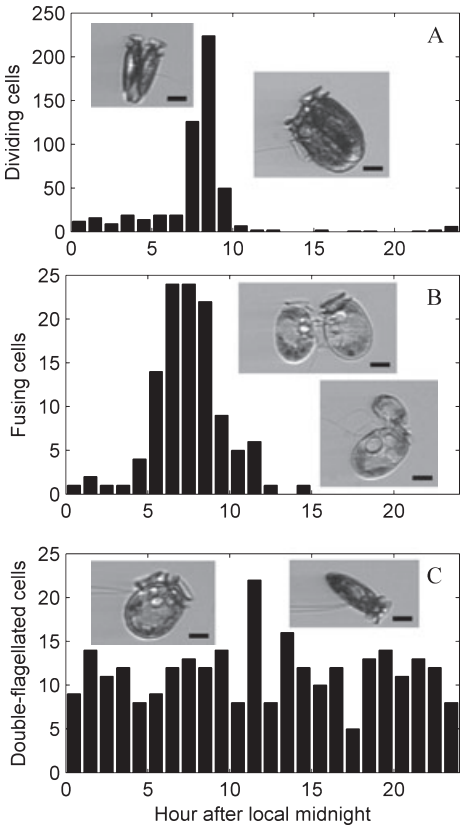

FIG. 5. Time of day when *Dinophysis* were observed in various life-cycle stages. For 28 selected days (see Fig. 6 for dates), all *Dinophysis* images were inspected manually, and the summed results presented as a function of time of day. (A) Dividing cells. (B) Fusing cells (putative gametes). (C) Possible planozygotes (cells with paired flagella). Scale bars = 10 μm.

DISCUSSION

Observations from the initial deployment of IFCB on the Texas coast provided early warning for a *Dinophysis* bloom that resulted in the first closure and recall of oyster harvests due to DSP in the U.S. (Texas State Department of Health Services). Closures ultimately extended far from the ship channel observation point, into Aransas, Corpus Christi, and Copano Bays. The alert occurred shortly before the Rockport Oysterfest, an annual event in the Port Aransas region that attracts up to 30,000 people, and so may have averted serious consequences to human health. *Dinophysis* as the causative agent for DSP was first reported in Japan (Yasumoto et al. 1980), and while *Dinophysis* blooms have been a recurring problem in Europe, Japan, and Korea, to our knowledge, there are no previous reports of *Dinophysis* being abundant in the Gulf of Mexico (Licea et al. 2004). This unexpected bloom reached >300 cells · mL^{-1}, which is among the highest cell concentrations reported for *Dinophysis* (Dahl and Johannessen 2001).

Variability in size and morphology among *Dinophysis* cells (Reguera and González-Gil 2001, Reguera et al. 2007, Escalera and Reguera 2008) makes it difficult to identify species based on images alone, but cells from this bloom most closely resembled *D. ovum* (B. Reguera, pers. comm.); *cox1* sequence data are consistent with this identification. The difficulty in resolving the taxonomy of this species complex (which includes *D. acuminata, D. sacculus,* and *D. ovum*) has been noted previously for observations in the Mediterranean (Koukaras and Nikolaidis 2004). As more cultures become available and sequencing of archived material is undertaken (Henrichs et al. 2008, Raho et al. 2008), identifications should become more accurate.

With observations from IFCB (long duration, high resolution), it should be possible to go beyond documenting occurrence of species of interest. It is possible to explore sources of bloom events, possible ecological links, and associated changes in community structure. In some ways, this is challenging

TABLE 1. Overall frequency of occurrence for visible cell-cycle and sexual-cycle stages in *Dinophysis* during 2-week periods in February–March 2008; time of day (hour after local midnight) when stages occurred.

					Time of day (h)	
	N	Dividing (%)	Fusing (%)	Planozygotes (%)	Division	Fusing
1–14 February	4,121	1.75 (0.20)*	1.24 (0.17)*	1.43 (0.18)*	6.0 (0.3, 6)[a]	7.5 (0.3, 8)
15–29 February	52,068	0.74 (0.04)*	0.08 (0.01)	0.23 (0.02)	8.7 (0.2, 9)	8.4 (0.3, 7)
1–15 March	24,771	0.27 (0.03)	0.06 (0.02)	0.22 (0.03)	7.8 (0.4, 9)	8.6 (0.5, 6)
16–31 March	6,990	0.11 (0.04)	0.06 (0.03)	0.57 (0.09)*	8.3 (1.0, 9)	8.3 (1.1, 7)

Results reflect manual inspection of all *Dinophysis* images collected on 28 d selected to span the period (same days as in Fig. 6). *N* is the total number of *Dinophysis* images (all stages including single vegetative cells) inspected in each period; other values are mean with standard error in parentheses; for time of day, mode value follows the standard error. Occurrence of planozygotes was not synchronized (see Fig. 5), so time of day is omitted here for that category.

*Significantly different from all other means in column.

[a]Significantly different from all other means in column except the last period.

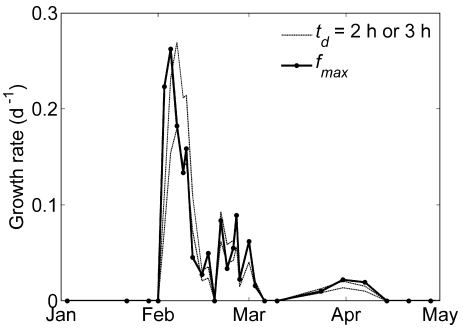

FIG. 6. Daily growth rate of *Dinophysis* spp. estimated from frequency of dividing cells on the subset of 28 d for which *Dinophysis* images were manually inspected to identify those dividing. Rates are shown according to the f_{max} approach and the mitotic index approach with two values of stage duration; higher and lower growth rate curves correspond to t_d =2 h and 3 h, respectively.

because a single-point time series is influenced by a variety of processes including advection in the presence of patchiness, vertical migration, and local growth and grazing. On the other hand, the strong currents through the narrow Port Aransas ship channel make it possible to sample a wide range of water masses (e.g., oceanic to estuarine) from a single location. We observed large changes in *Dinophysis* abundance at tidal frequencies, suggesting that spatial gradients were present (Fig. 4). Because we sampled from only one depth in the water column, vertical layering of cells could have produced a relationship between tidal flows and cell abundance, but this explanation seems unlikely since the shipping channel experiences tidal currents as high as 4 knots and the water column was well mixed (Min 2008) during the study period. The tidal frequency cell abundance changes probably reflect horizontal gradients in and out of the estuary, which may provide information about the origin of the bloom.

Possible origins of the *Dinophysis* bloom in the Mission-Aransas estuary include local seeding, introduction via ship ballast water, or transport of an offshore population. Although *Dinophysis* benthic resting cysts have been reported (Reguera et al. 2003), local seeding from the estuary seems unlikely as the bloom source because *D.* cf. *ovum* has not been reported previously in the Mission-Aransas estuary area. During the 2 months prior to the event, ships from Northern Europe and Brazil arrived in Corpus Christi (U.S. Coast Guard, Corpus Christi, pers. comm.) and could have introduced cells via ballast water (Hallegraeff 1998), but we have no evidence to support this source. Although *Dinophysis* blooms historically have not been observed in the Gulf of Mexico, the most likely source was an offshore population. Following the early warning provided by IFCB observations in February, retrospective analysis of archived samples collected from offshore during early 2008 revealed

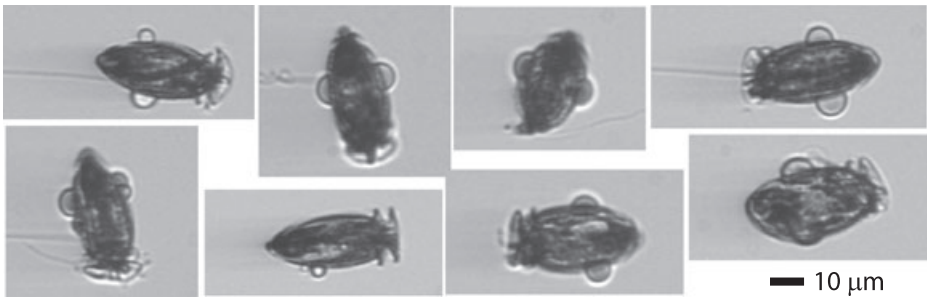

FIG. 7. Selected IFCB images from 27 February 2008 showing bubble-like structures. IFCB, Imaging FlowCytobot.

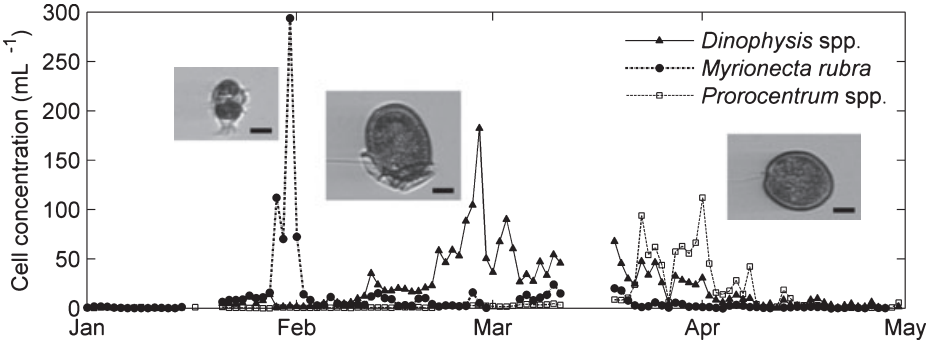

FIG. 8. Daily mean cell abundances for *Dinophysis* spp., *Myrionecta rubra*, and *Prorocentrum* spp. during January–May 2008. Standard errors for daily binned results (computed following the method of Solow et al. 2001 as in Sosik and Olson 2007) were <1, <1.5, and <0.73 cell · mL^{-1} for *Dinophysis, Myrionecta*, and *Prorocentrum*, respectively; all values are very small and so are omitted for clarity. Scale bars = 10 μm.

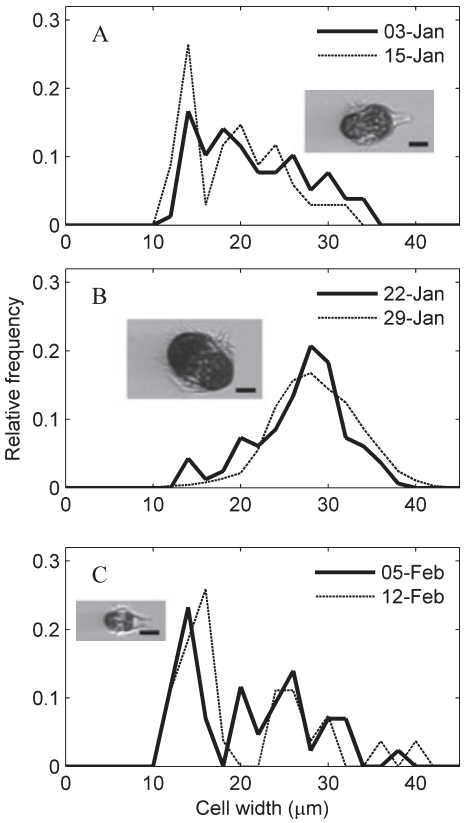

FIG. 9. Daily mean normalized size distributions for *Myrionecta rubra* for three time periods in January–February 2008. Automated image classification results were manually corrected for false positives prior to constructing distributions, which are based on short axis lengths (cell width) estimated from automated image processing. To facilitate comparison of shapes, distributions are scaled by the total number of *M. rubra* observed on each day. (A) 3 January ($n = 78$) and 15 January ($n = 34$); (B) 22 January ($n = 164$) and 29 January ($n = 9{,}332$); (C) 5 February ($n = 43$) and 12 February ($n = 27$). Scale bars = 10 μm.

elevated abundance of *Dinophysis* (up to 26 cell · mL^{-1}) at several sites along the Texas coast from the Louisiana border to Mexico, including the region near the UTMSI pier site (Swanson 2008). In addition, during the 10 d before the bloom peak, our observations show that cell abundance increased when the current was flowing into the estuary, consistent with an offshore origin (Fig. 4). It seems likely that local growth or concentrating mechanisms within the estuary also contributed to the bloom evolution since cell concentrations at the ship channel reached levels >10-fold those reported offshore, and even higher concentrations were reported inside the estuary (Texas State Department of Health Services).

The IFCB observations provide information about biological factors that can influence bloom evolution, including the proportions of cells in different life-history stages. The relative frequencies of dividing cells, fusing cells, and putative planozygotes were all highest in the early part of the bloom (Table 1) and were of comparable magnitudes. Dividing and fusing cells only occurred during morning hours, when they could be up to 5%–8% of the population. Peak levels of planozygotes were lower, but they were present throughout the day such that their overall occurrence was similar to the other stages during early February (1%–2% of the population). The frequency of occurrence for all of these stages (dividing, fusing, and planozygotes) declined in the second half of February, but the drop was less abrupt for dividing cells. This result may indicate that vegetative growth continued, while entry into sexual stages of the life cycle largely stopped. There was a significant increase in the presence of planozygotes again during the last half of March, which might indicate renewed sexual activity during unfavorable conditions as the bloom declined during this period (Fig. 2). The occurrence of planozygotes throughout the event is similar to observations for *D. acuminata* in Brittany waters by Gentien et al. (2004 cited in Reguera et al. 2007). This life-history stage has rarely been studied in natural populations because the paired flagella that help identify planozygotes do not preserve well (McLachlan 1993, cited in Reguera et al. 2007) and are best observed in live cells (as by IFCB).

The time-series observations of dividing cells allowed division rates to be estimated at different points in the bloom: growth was fastest at the onset of the bloom and decreased as the peak in abundance was approached. Our estimates of division rates for *D.* cf. *ovum* (Fig. 6) are similar to estimates in previous reports for species within the *D. acuminata* species complex (Garcés et al. 1997). While the f_{max} and mitotic index approaches gave similar results, it should be noted that each is subject to uncertainty. The f_{max} approach will produce underestimates if the duration of the paired-cell stage is shorter than the division burst (McDuff and Chisholm 1982), and the ''mitotic cell index'' growth rate calculations depend directly on the assumed duration of the paired-cell stage, for which we have only indirect evidence. The observed timing of the cell-division burst shifted significantly during the bloom, from 06:00 in the initial stage to 08:00–09:00 afterward (Table 1). We cannot explain this shift, but the fact that the cell-division process is variable emphasizes that we also cannot be sure the duration of the stage is constant over the bloom.

The kleptoplastidic ciliate *M. rubra*, a known prey item of *Dinophysis* (Park et al. 2006), has been reported to vary seasonally, with maximum abundance up to 50 cells · mL^{-1} (Witek 1998). We observed considerably higher concentrations, up to 300 cells · mL^{-1} during the last week of January (Fig. 8). High concentrations of *M. rubra* lasted only a few days, after which *Dinophysis* abundances began to increase and growth rates were high for more than a week (Fig. 6). Because this is a dynamic coastal regime and sampling occurred at only one

location, we cannot be sure that these events are directly linked, but it is evident that patches of abundant *M. rubra* occurred, and it is possible that these allowed rapid growth of *Dinophysis*. Several studies have documented that various *Dinophysis* species grow mixotrophically, maintaining for several generations photosynthetically active plastids obtained from *M. rubra* (Park et al. 2006, 2008, Kim et al. 2008). *D. acuminata* has been shown to grow in the absence of prey for a week or more at rates similar to those we observed in early February (Kim et al. 2008), whereas studies of *D. caudata* have shown they can grow photosynthetically for more than a month after feeding.

Notably, we observed dramatic changes in size of *M. rubra*: at their peak in abundance, *M. rubra* cells were nearly twice as large as before or after (Fig. 9). Wide variations in *M. rubra* cell-size distributions have been noted previously and attributed to seasonal variations in nutrients and prey availability rather than presence of multiple strains (Montagnes et al. 2008).

The bubble-like features that appeared on up to 4% of the *Dinophysis* cells IFCB sampled during the outgoing tide on 27 February (the day of the peak in cell abundance) were only rarely observed in the rest of the data set, which makes it difficult to deduce their cause. These structures, which to our knowledge have never been reported in a natural population, have previously been observed in laboratory cultures of *D. acuminata*, where it seems they may represent a response to stress: Park et al. (2006) saw them after the cells had been feeding on *M. rubra*, but their cause was likely the bright lights required for the observations (M. Park, pers. comm.), and other workers have seen such features during early stages of culturing from manually isolated cells, before the cultures were actively growing and feeding (D. Kulis, M. Tong, pers. comm.).

The period on 27 February when IFCB observations showed cells with bubbles was clearly demarcated by abrupt changes in cell abundance (data not shown), suggesting that we were sampling a distinct population that may have been stressed. It is also worth noting that the ''bubbles'' resemble ''blebs,'' which are poorly understood features of many cell types (Charras 2008) the function of which is, in most cases, unknown but which have been suggested to play a part in such processes as division and apoptosis.

The ''bloom'' of *Prorocentrum* spp. that followed the toxic *Dinophysis* event did not appear to contribute to oyster toxicity, as the DSP warning was lifted in mid-April (J. R. Deeds, K. Wiles, G. B. Heideman VI, K. D. White, and A. Abraham, unpublished data). Co-occurrence of *Prorocentrum* spp. with *Dinophysis* spp. also was observed in Narragansett Bay (Maranda and Shimizu 1987) and in the NW Mediterranean (Jamet et al. 2005). The timing of blooms of *D. acuminata* and *D.* cf. *ovum* (March) is also similar between the Gulf of Mexico in 2008 and the Mediterranean in 2000 and 2002 (Koukaras and Nikolaidis 2004).

The reasons for success of one species, or species assemblage, over another are poorly understood (GEOHAB 2003, HARRNESS 2005). Detailed time-series data as from IFCB can help us to address such questions about relationships among species, as well as about the mechanisms behind bloom dynamics, such as the timing of gamete production and fusion, and perhaps even cell death.

CONCLUSION

IFCB provided early warning of the first toxic *Dinophysis* bloom detected in the U.S. Continuous monitoring allowed detection of cell concentrations above typical background levels, which led to further sampling to confirm the presence of OA toxin in water and oyster samples from Port Aransas harbor and adjacent bays, and the early warning and timely closure of shellfish harvesting prevented human illness. This successful event response demonstrated that monitoring can be guided by continuous automated methods to provide real-time detection of a HAB event. The high temporal resolution and long duration of the automated observations enhance our ability to observe the abundance of individual phytoplankton taxa at temporal scales relevant for better understanding of community dynamics, predator-prey interactions, and prediction of HABs.

We thank E. Quiroz, S. Lanoux, Marc Teller, and staff at UTMSI for their assistance and support in setting up field operation, J. Corn for maintenance in keeping IFCB running, J. Hamm for help with manual classification, and H. R. Granade for LC–MS technical assistance. We also thank B. Reguera, K. Steidinger, and A. Zingone for examining images. Funding for this research was provided by CICEET–07-025 to R. J. O., H. M. S., and L. C. University of Texas Marine Science Institute Contribution number 1508.

Buskey, E. J. & Hyatt, C. J. 2006. Use of the FlowCAM for semi-automated recognition and enumeration of red tide cells (*Karenia brevis*) in natural plankton samples. *Harmful Algae* 5:685–92.

Campbell, L., Walpert, J. N. & Guinasso, N. L., Jr. 2008. A new buoy-based *in situ* optical early warning system for harmful algal blooms in the Gulf of Mexico. *Nova Hedwigia Suppl.* 133:161–70.

Carpenter, E. J. & Chang, J. 1988. Species-specific phytoplankton growth rates via diel DNA synthesis cycles. I. Concept of the method. *Mar. Ecol. Prog. Ser.* 43:105–11.

CENR. 2000. *National Assessment of Harmful Algal Blooms in US Waters.* National Science and Technology Council Committee on Environment and Natural Resources, Washington, D.C., 38 pp.

Charras, G. T. 2008. A short history of blebbing. *J. Microsc. (Oxf.)* 231:466–78.

Dahl, E. & Johannessen, T. 2001. Relationship between occurrence of *Dinophysis* species (Dinophyceae) and shellfish toxicity. *Phycologia* 40:223–7.

Escalera, L. & Reguera, B. 2008. Planozygote division and other observations on the sexual cycle of several species of *Dinophysis* (Dinophyceae, Dinophysiales). *J. Phycol.* 44:1425–36.

Garcés, E., Delgado, M. & Camp, J. 1997. Phased cell division in a natural population of *Dinophysis sacculus* and the *in situ* measurement of potential growth rate. *J. Plankton Res.* 19:2067–77.

Gentien, P., Lazure, P., Ne′zan, E., Lunven, M., Crassous, M. P. & Danie′lou, M. M. 2004. How do the gametes of the rare marine protist *Dinophysis acuminata* mate? *In Programme and Abstracts of the XI International Conference on Harmful Algae, Cape Town, South Africa, 14–19 November 2004,* p. 121.

GEOHAB. 2003. *Global Ecology and Oceanography of Harmful Algal Blooms, Implementation Plan*. Gentien, P., Pitcher, G., Cembella, A. & Glibert, P. [Eds.] SCOR and IOC, Baltimore and Paris, 36 pp.

Giacobbe, M. G. & Gangemi, E. 1997. Vegetative and sexual aspects of *Dinophysis pavillardi* (Dinophyceae). *J. Phycol.* 33:73–80.

Hallegraeff, G. M. 1998. Transport of toxic dinoflagellates via ships' ballast water: bioeconomic risk assessment and efficacy of possible ballast water management strategies. *Mar. Ecol. Prog. Ser.* 168:297–309.

HARRNESS. 2005. *Harmful Algal Research and Response: A National Environmental Science Strategy 2005–2015*. Ramsdell, J. S., Anderson, D. M. & Glibert, P. M. [Eds.] Ecological Society of America, Washington, D.C., 96 pp.

Henrichs, D. W., Renshaw, M. A., Santamaria, C. A., Richardson, B., Gold, J. R. & Campbell, L. 2008. PCR amplification of microsatellites from single cells of *Karenia brevis* preserved in Lugol's iodine solution. *Mar. Biotech.* 10:122–7.

Jamet, J. L., Jean, N., Boge, G., Richard, S. & Jamet, D. 2005. Plankton succession and assemblage structure in two neighbouring littoral ecosystems in the north-west Mediterranean Sea. *Mar. Freshw. Res.* 56:69–83.

Kim, S., Kang, Y. G., Kim, H. S., Yih, W., Coats, D. W. & Park, M. G. 2008. Growth and grazing responses of the mixotrophic dinoflagellate *Dinophysis acuminata* as functions of light intensity and prey concentration. *Aquat. Microb. Ecol.* 51:301–10.

Koukaras, K. & Nikolaidis, G. 2004. *Dinophysis* blooms in Greek coastal waters (Thermaikos Gulf, NW Aegean Sea). *J. Plankton Res.* 26:445–57.

Licea, S., Zamudio, M. E., Luna, R. & Soto, J. 2004. Free-living dinoflagellates in the southern Gulf of Mexico: report of data (1979–2002). *Phycol. Res.* 52:419–28.

Lin, S. J., Zhang, H. A., Spencer, D. F., Norman, J. E. & Gray, M. W. 2002. Widespread and extensive editing of mitochondrial mRNAs in dinoflagellates. *J. Mol. Biol.* 320:727–39.

Maranda, L. & Shimizu, Y. 1987. Diarrhetic shellfish poisoning in Narragansett Bay. *Estuaries* 10:298–302.

McDuff, R. E. & Chisholm, S. W. 1982. The calculation of *in situ* growth rates of phytoplankton populations from fractions of cells undergoing mitosis: a clarification. *Limnol. Oceanogr.* 27:783–8.

McLachlan, J. L. 1993. Evidence for sexuality in a species of *Dinophysis*. *In* Smayda, T. J. & Shimizu, Y. [Eds.] *Toxic Phytoplankton Blooms in the Sea*. Elsevier, Amsterdam, pp. 143–6.

McNabb, P., Selwood, A. I. & Holland, P. T. 2005. Multiresidue method for determination of algal toxins in shellfish: single-laboratory validation and interlaboratory study. *J. AOAC Int.* 88:761–72.

Min, D. 2008. High frequency and multi-parameter observation of land-sea connection at the Aransas Pass tidal inlet, south Texas in Summer 2008. *EOS Trans. AGU* 89(53) Fall Meet. Suppl. Abstract OS21C–1196.

Montagnes, D., Allen, J., Brown, L., Bulit, C., Davidson, R., Diaz-Avalos, C., Fielding, S., et al. 2008. Factors controlling the abundance and size distribution of the phototrophic ciliate *Myrionecta rubra* in open waters of the North Atlantic. *J. Eukaryot. Microbiol.* 55:457–65.

Olson, R. J. & Sosik, H. M. 2007. A submersible imaging-in-flow instrument to analyze nano-and microplankton: Imaging FlowCytobot. *Limnol. Oceanogr. Methods* 5:195–203.

Park, M. G., Kim, S., Kim, H. S., Myung, G., Kang, Y. G. & Yih, W. 2006. First successful culture of the marine dinoflagellate *Dinophysis acuminata*. *Aquat. Microb. Ecol.* 45:101–6.

Park, M. G., Park, J. S., Kim, M. & Yih, W. 2008. Plastid dynamics during survival of *Dinophysis caudata* without its ciliate prey. *J. Phycol.* 44:1154–63.

Raho, N., Pizarro, G., Escalera, L., Reguera, B. & Marin, I. 2008. Morphology, toxin composition and molecular analysis of *Dinophysis ovum* Schutt, a dinoflagellate of the ''*Dinophysis acuminata* complex.'' *Harmful Algae* 7:839–48.

Reguera, B., Garces, E., Pazos, Y., Bravo, I., Ramilo, I. & Gonzalez-Gill, S. 2003. Cell cycle patterns and estimates of *in situ* division rates of dinoflagellates of the genus *Dinophysis* by a postmitotic index. *Mar. Ecol. Prog. Ser.* 249:117–31.

Reguera, B. & González-Gil, S. 2001. Small cell and intermediate cell formation in species of *Dinophysis* (Dinophyceae, Dinophysiales). *J. Phycol.* 37:318–33.

Reguera, B., Gonzalez-Gil, S. & Delgado, M. 2007. *Dinophysis diegensis* is a life history stage of *Dinophysis caudata* (Dinophyceae, Dinophysiales). *J. Phycol.* 43:1083–93.

Solow, A., Davis, C. & Hu, Q. 2001. Estimating the taxonomic composition of a sample when individuals are classified with error. *Mar. Ecol. Prog. Ser.* 216:309–11.

Sosik, H. M. & Olson, R. J. 2007. Automated taxonomic classification of phytoplankton sampled with imaging-in-flow cytometry. *Limnol. Oceanogr. Methods* 5:204–16.

Sosik, H. M, Olson, R. J. & Armbrust, E. V. 2010. Flow cytometry in plankton research. *In* Suggett, D., Prasil, O. & Borowitzka, M. A. [Eds.] *Chlorophyll a Fluorescence in Aquatic Sciences: Methods and Applications*. Springer, Dordrecht, the Netherlands (in press).

Suttle, C. A. 1993. Enumeration and isolation of viruses. *In* Kemp, P. F., Sherr, B. F., Sherr, E. B. & Cole, J. J. [Eds.] *Handbook of Methods in Aquatic Microbial Ecology*. Lewis Publishers, Boca Raton, Florida, pp. 121–34.

Swanson, K. M. 2008. The 2008 Texas *Dinophysis acuminata* bloom: distribution and toxicity. MS thesis, The University of Texas at Austin, 101 pp.

Tango, P., Butler, W., Lacouture, R., Goshorn, D., Magnien, R., Michael, B., Hall, H., Browhawn, K., Wittman, R. & Betty, W. 2004. An unprecedented bloom of *Dinophysis acuminata* in Chesapeake Bay. *In* Steidinger, K. A., Landsberg, J. A., Tomas, C. R. & Vargo, G. A. [Eds.] *Harmful Algae 2002—Proceedings of the Xth International Conference on Harmful Algae*. Florida Fish and Wildlife Conservation Commission, Florida Institute of Oceanography, St. Petersburg, Florida, and IOC-UNESCO, Paris, pp. 358–63.

Vaulot, D. 1992. Estimate of phytoplankton division rates by the mitotic index method – the f_{max} approach revisited. *Limnol. Oceanogr.* 37:644–9.

Witek, M. 1998. Annual changes of abundance and biomass of planktonic ciliates in the Gdansk Basin, southern Baltic. *Int. Rev. Hydrobiol.* 83:163–82.

Yasumoto, T., Murata, M., Oshima, Y., Sano, M., Matsumoto, G. K. & Clardy, J. 1985. Diarrhetic shellfish toxins. *Tetrahedron* 41:1019–25.

Yasumoto, T., Oshima, Y., Sugawara, W., Fukuyo, Y., Oguri, H., Igarashi, T. & Fujita, N. 1980. Identification of *Dinophysis fortii* as the causative organism of diarrhetic shellfish poisoning. *Bull. Jpn. Soc. Sci. Fish.* 46:1405–11.

Supplementary Material

The following supplementary material is available for this article:

Figure S1. Chromatogram for (A) *Dinophysis* bloom seawater sample (B) okadaic acid and dinophysis toxin–1 (DTX-1) reference standards.

This material is available as part of the online article.

Please note: Wiley-Blackwell are not responsible for the content or functionality of any supplementary materials supplied by the authors. Any queries (other than missing material) should be directed to the corresponding author for the article.